GLOBAL EJECTA FROM CHICXULUB: SPHERULES, SHOCKED QUARTZ, AND MORE. N. Artemieva[1,2] and J. Morgan[3], [1]Planetary Science Institute 85719 Tucson, [2]Institute for Dynamics of Geospheres 119334 Moscow, artemeva@psi.edu, [3]Imperial College London, UK, j.morgan@imperial.ac.uk

Introduction: The K-Pg boundary is widely recognized as a global ejecta layer formed by a large meteorite impact 65 million years ago. The discovery of an iridium anomaly [1], shocked quartz grains [2], and the Chicxulub crater [3] provided the strongest confirmation of the impact hypothesis. However, 30 years later the mechanism for transporting the impact ejecta world-wide is still unclear, and atmospheric disturbances may play a crucial role in ejecta re-distribution [4-6]. With this in mind we now face a new challenge: to model the Chicxulub ejecta starting from impact and ending with the deposition of the ejecta (shocked quartz and spherules) around the globe. To solve this problem we have to deal with extremely different time and spacial scales: from seconds to days, and from microns to thousands of km.

Numerical model: We model the impact with the 3D hydrocode SOVA [7] complemented by the ANEOS equation of state for geological materials [8]. In three separate stages we model: 1) the impact and initial ejection of material; 2) the ballistic continuation of ejecta on a spherical earth; and 3) ejecta as it re-enters the atmosphere.

The modeled Chicxulub target consists of a 3-km-thick sedimentary layer (porous water-saturated limestone), a 30-km-thick crystalline basement (granite), and mantle (dunite). We vary the projectile size from 13 to 16 km and impact angle from 30 to 60°, whilst keeping the transient cavity diameter constant and equal to 90-100 km, in accordance with estimates for Chicxulub [6]. Impact angles outside this range are less likely, and highly oblique and near-vertical impacts appear to be unable to reproduce the total mass and meteoritic composition of the K-Pg layer [6].

Tracers are used to track particles to an altitude of 100 km and quantify the mass of ejected material, its depth of origin, maximum shock compression and velocity. The ejecta is then assumed to continue on a ballistic path around the earth, and the location and time of re-entry is determined for each tracer. At an altitude of 100 km re-entering tracers are replaced by real particles with a size-frequency distribution in accordance with their maximum shock pressure [9]. The interaction of these particles with the atmosphere is modeled using a multi-phase approximation and a spherical earth.

Results: The thickness of ejecta arriving at the top of the atmosphere for a 45° impact angle is shown in Fig. 1. As expected, ejecta thickness decreases quickly with increasing distance from the crater, is highly asymmetric, and thickens at the antipode (~20,000 km). The modeled ejecta thickness in the downrange direction (red curve) is substantially higher than observed at the K-Pg boundary in any direction from Chicxulub. Three possible reasons for this are: 1) the ejecta may be substantially re-distributed by atmospheric flows during re-entry (see next section); 2) the impact angle was steeper and, hence, the ejecta distribution was less asymmetric; 3) sedimentary ejecta may be subjected to thermal decomposition during impact or re-entry, meaning that only a portion of the sediments would be deposited in the K-Pg layer.

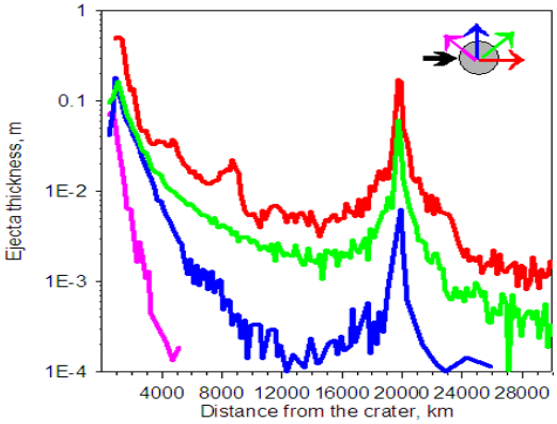

Fig.1. Ejecta thickness at the top of the atmosphere versus distance for a 45° impact. Color indicates azimuth: red is downrange, green 45°, blue 90° and pink 135°.

For all distances from the crater we also estimate changes in the re-entering ejecta with time (Fig. 2).

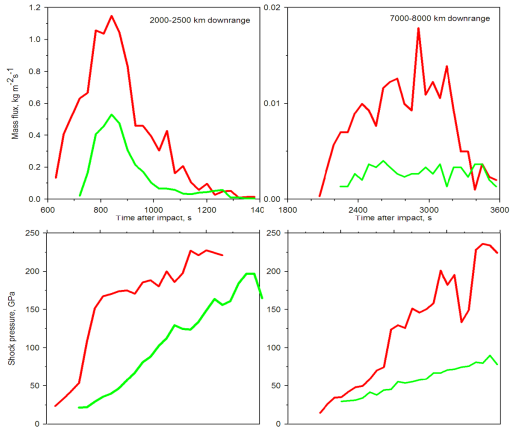

Fig.2. The mass flow (top) and maximum shock pressure (bottom) at distances of 2000-2500 km (left) and 7000-8000 km (right). Red is downrange, green is 45°.

At all sites the early arriving ejecta have been subjected to lower shock pressures (some sediments remain solid), arrive with lower velocity and at shallower re-entry angles (40-60°). Late ejecta have been compressed to pressures in excess of 150 GPa (thus are partially vaporized), have higher velocities, steeper re-entry angles, and a high projectile content. At distal sites the calculated mass flux is higher, but shorter in duration, than previously estimated values [5, 10].

Analysis: We examine the ejecta distribution over velocity, mass, ejection angle to find the reason for the differences between our model and previous models. We note that, although an impact plume does form above the growing crater, the majority of the ejecta is within the ejecta curtain – not the plume. In our model 80-90% of the distal ejecta is ejected at angles of between 40-60°, including some high-velocity ejecta. These materials arrive at the top of the atmosphere around the globe at about the same time. Our model differs to previous models that assume the ejecta is distributed evenly in a hemispherical plume [5, 10].

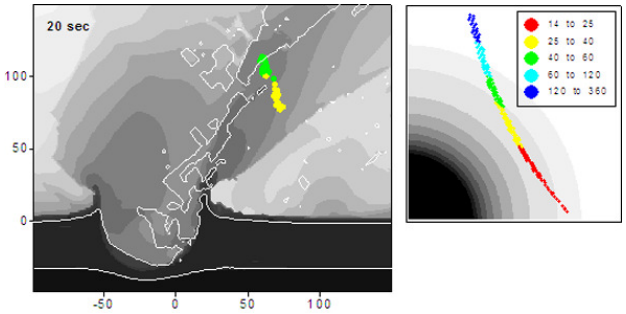

Fig.3. Comparison of the modeled plume on the left with a hypothetical plume [10] on the right. The modeled plume is highly diluted (light gray) in its central part, and most ejected material lies within the ejecta curtain. Colored tracers show materials which will be deposited at the angular distances of 54-60° (6000-6700 km). Colors correspond to the time of deposition in minutes (see legend).

Atmospheric disturbances and non-ballistic redistribution of ejecta: Up to distances of 1000 km from the crater ejecta are deposited ballistically within the first 20 minutes. At larger distances interaction of ejecta with the atmosphere plays an important role: ejecta density currents are formed (although they never reach the surface as they disappear during descent), fine ejecta are thrown back upwards to the rarified atmosphere, and strong atmospheric shock waves disperse ejecta in all directions. Two hours after the impact 99% of ejecta have been deposited (Fig. 4). The remaining particles (still in the atmosphere) have sizes from 1 μm (1.5 % of the total non-deposited mass), 10 μm (18%), and 100 μm (80%). These long-lasting ejecta contain particles from all target units (i.e. shocked quartz grains from the basement, sulfur aerosols from the sedimentary cover) and plenty of the projectile material (which was partially vaporized during the impact). On average, smaller particles are further from the crater, at higher altitude, and have higher velocities (horizontally and vertically). Whilst the upper atmosphere (above ~50 km) is still strongly disturbed (horizontal velocities reach a couple of km/s, i.e. much bigger than any hurricanes), the lower atmosphere is almost quiet.

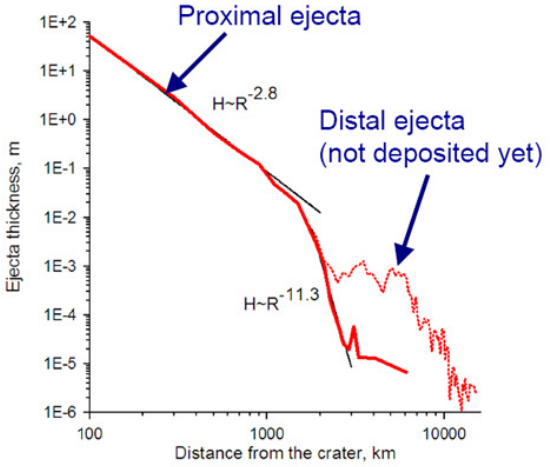

Fig. 4. Ejecta thickness as a function of distance from the crater ~ 2 hours after impact. Solid line shows already deposited particles, dashed – all ejecta, assuming immediate vertical sedimentation of the finest particles, which are in the atmosphere.

Discussion: Atmospheric disturbances are caused by ejecta re-entry and are expected for all large-scale impacts. Ejecta-atmosphere coupling depends on the particles' size-frequency distribution, which is still unknown (especially for the smallest particles, products of multi-staged fragmentation and condensation from the plume). A real impact plume may be much more complicated due to fractionation of materials with different melting and vaporization temperatures. At high altitudes viscosity may be important and should include not only standard Newtonian viscosity, but also ionic drag. These results may be used to model the level and duration of radiation on the earth's surface.

References: [1] Alvarez L.W. et al. (1980) *Science 208*, 1095-1108. [2] Bohor B. et al. (1984) *Science 224*, 867-869. [3] Hildebrand A.R. et al. (1991) *Geology 19*, 867-871. [4] Colgate S. A. and A. G. Petschek (1985) *LA-UR-84-3911*, Los Alamos Natl. Lab., NM. [5] Goldin T. and H. J. Melosh (2009) *Geology 37,* 1135-1138. [6] Artemieva N, and Morgan J. (2009) *Icarus 201,* 768-780. [7] Shuvalov V. (1999) *Shock waves 9*, 381-390. [8] Thompson S.L. and Lauson H.S. (1972) *SC-RR-61 0714.* Sandia Nat. Lab., Albuquerque, NM. 119 p. [9] Artemieva N. and Ivanov B. (2004*) Icarus 71*, 84-101. [10] Melosh et al. (1990) *Nature 343*: 251-254.